

Investigating Singularities of the Observability Jacobian for Nonlinear Power Systems

C. J. Dafis, *Member, IEEE*, and C. O. Nwankpa, *Member, IEEE*

Abstract— This paper focuses on computing and interpreting the significance of the observability Jacobian singularities. Previous efforts have focused on developing an observability index and determining the effects of model/measurement changes to the observability formulation. Using this index, the singularities of the Jacobian are extracted, and preliminary results indicate that there is a duality between the loss of stability (whether it be phase or voltage stability), and the loss of observability. Thus, providing a single dual-use metric capable of forecasting both stability and observability characteristics of a system. The results are illustrated using a sample 3-bus system.

Index Terms—observability, power systems, system index, differential algebraic equations.

I. INTRODUCTION

The safe, reliable and economic operation of modern power systems rely on increased levels of system automation, power electronic equipment, and system controllers capable of monitoring and controlling the system through various operating points.

One particular family of power systems where the effects of system automation, power converters and rapid system reconfiguration are more profound are naval shipboard power systems. The inherent nature of the shipboard systems, similar to island topologies in terrestrial systems, has magnified the need for real-time system control and therefore the development of dynamic state estimators and nonlinear observers. Shipboard power systems are unique in their composition, and differ from terrestrial systems in many ways [1]:

- Single dynamic loads consuming a large portion of the generation capacity
- Time constants of the generators are closer to the electrical time constants than in terrestrial systems
- System reconfiguration routines are much faster and a large portion of the system load is sensitive to power interruptions. A small interruption of approximately 100 msec. can cause subsystems to shut-down.
- Redundancy is incorporated in all aspects of system design

to ensure survivability

The power demand on a ship has evolved from kilowatts the tens of megawatts, and is constantly increasing with new ship designs and concepts. One particular concept affecting directly the shipboard power system is the vision for an All Electric Ship [2], which signifies the move of the shipboard power system from an electromagnetic/electromechanical basis to a power electronic basis. Some of the design aspects involving the All Electric Ship concept are:

- Electric Drive
- Integrated Power System
- Zonal Distribution System
- Reduced Manning

The enabling technology in all of the above concepts is intelligent automation and control. With the increase in the automation of system functions within the shipboard power system, the dependence on both executive and distributed controllers to maintain the performance of the power system at acceptable levels is becoming more apparent. Traditional control approaches based on linearized models of the system generation/distribution capacity will not be sufficient. The need of incorporating the nonlinear dynamics of the shipboard power system in the control methodology is the solution to this problem, and one proposed solution is the use of nonlinear observer based controllers and dynamic state estimators. Before these solutions are designed however, the concept of nonlinear observability is first investigated. Providing an implementation of the observability formulation for power systems modeled as Differential Algebraic Equations is the starting point for the development of nonlinear controllers, dynamic state estimators and performance index measures.

The authors have investigated the problem of system observability for nonlinear power systems modeled as DAEs [3-6], and this work emphasizes on the possible duality between the singularities of the observability Jacobian and the known stability characteristics of the system. The preliminary results indicate that a system becomes unobservable at the maximum load point.

II. PROBLEM FORMULATION

The majority of the system models used in this work and presented in this section are adopted from [4] and repeated here for the sake of continuity. The Differential Algebraic Model of a power system consisting of n generators and m

This work was supported in part by the (NAVSEA-ILIR), under grant number 051911353510 and the Department of Energy under grant number CH11171.

C. J. Dafis is with NAVSEA-Philadelphia, Philadelphia, PA 19112 USA (dafiscj@nswccd.navy.mil)

C. O. Nwankpa is director of CEPE, Drexel University, Philadelphia, PA 19104 USA (chika@nwankpa.ece.drexel.edu)

Report Documentation Page				Form Approved OMB No. 0704-0188	
Public reporting burden for the collection of information is estimated to average 1 hour per response, including the time for reviewing instructions, searching existing data sources, gathering and maintaining the data needed, and completing and reviewing the collection of information. Send comments regarding this burden estimate or any other aspect of this collection of information, including suggestions for reducing this burden, to Washington Headquarters Services, Directorate for Information Operations and Reports, 1215 Jefferson Davis Highway, Suite 1204, Arlington VA 22202-4302. Respondents should be aware that notwithstanding any other provision of law, no person shall be subject to a penalty for failing to comply with a collection of information if it does not display a currently valid OMB control number.					
1. REPORT DATE JUL 2005		2. REPORT TYPE		3. DATES COVERED 00-00-2005 to 00-00-2005	
4. TITLE AND SUBTITLE Investigating Singularities of the Observability Jacobian for Nonlinear Power Systems				5a. CONTRACT NUMBER	
				5b. GRANT NUMBER	
				5c. PROGRAM ELEMENT NUMBER	
6. AUTHOR(S)				5d. PROJECT NUMBER	
				5e. TASK NUMBER	
				5f. WORK UNIT NUMBER	
7. PERFORMING ORGANIZATION NAME(S) AND ADDRESS(ES) Naval Surface Warfare Center -Carderock Division,NAVSEA-Philadelphia,Philadelphia,PA,19112				8. PERFORMING ORGANIZATION REPORT NUMBER	
9. SPONSORING/MONITORING AGENCY NAME(S) AND ADDRESS(ES)				10. SPONSOR/MONITOR'S ACRONYM(S)	
				11. SPONSOR/MONITOR'S REPORT NUMBER(S)	
12. DISTRIBUTION/AVAILABILITY STATEMENT Approved for public release; distribution unlimited					
13. SUPPLEMENTARY NOTES See also ADM001931. Proceedings of the 2005 IEEE Electric Ship Technologies Symposium (ESTS 2005) Held in Philadelphia, PA on July 25-27, 2005.					
14. ABSTRACT see report					
15. SUBJECT TERMS					
16. SECURITY CLASSIFICATION OF:			17. LIMITATION OF ABSTRACT Same as Report (SAR)	18. NUMBER OF PAGES 6	19a. NAME OF RESPONSIBLE PERSON
a. REPORT unclassified	b. ABSTRACT unclassified	c. THIS PAGE unclassified			

static load buses is given as:

$$\begin{aligned} \dot{x} &= f(x, u, N) & f: \mathbb{R}^{2(n+m-1)} &\rightarrow \mathbb{R}^{2(n-1)} \\ 0 &= g(x, u, N) & g: \mathbb{R}^{2(n+m-1)} &\rightarrow \mathbb{R}^{2(m)} \\ y &= h(x, N) & h: \mathbb{R}^{2(n+m-1)} &\rightarrow \mathbb{R}^r \end{aligned} \quad (1)$$

where $f(\cdot)$ is the set of differential equations related to the dynamics of the generation equipment, $g(\cdot)$ is the set of nonlinear algebraic equations related to the static load buses of the system, $h(\cdot)$ are the measurement equations, u are the system inputs, N describes the characteristics of the individual power lines in the system, x is the system vector containing both the dynamic states and static variables of the system, and y are the available measurements. More information on DAE power system models and their related characteristics can be found in [7].

By reformulating (1) in a more condensed version:

$$\begin{aligned} F(\dot{x}, x, N) &= Bu \\ y &= h(x, N) \end{aligned} \quad (2)$$

the observability Jacobian (J_o) of the system is given by [8]:

$$J_o = \begin{bmatrix} G_x & G_{\dot{x}} & G_w \\ H_x & H_{\dot{x}} & H_w \end{bmatrix} \quad (3)$$

where

$$\begin{aligned} G &= \begin{bmatrix} F(\dot{x}, x, N) \\ F^{(1)} : F_x(\dot{x}, x, N)\dot{x} + F_{\dot{x}}(\dot{x}, x, N)\ddot{x} \\ \vdots \\ F^{(s)} : (F(\dot{x}, x, N))^{(s)} \end{bmatrix} \\ H &= \begin{bmatrix} h(x, N) \\ h^{(1)} : h_x(x, N)\dot{x} \\ \vdots \\ h^{(r)} : h(x, N)^{(r)} \end{bmatrix} = \begin{bmatrix} y \\ y^{(1)} \\ \vdots \\ y^{(r)} \end{bmatrix} \end{aligned} \quad (4)$$

and s is the system differentiation index, r is the measurement differentiation index, and w are the higher derivatives of x ($2 \dots w$). Based on this Jacobian, the system is said to be smoothly observable if [8]:

$$\begin{aligned} 1. \quad \text{rank}(J_o) &= n + \text{rank} \begin{bmatrix} G_{\dot{x}} & G_w \\ H_{\dot{x}} & H_w \end{bmatrix} \\ 2. \quad \text{rank}(J_o) &\text{ is constant rank on } S \\ S: \{0 &= g(x, u, N)\} \end{aligned} \quad (5)$$

A. Power System Model

In the adopted structure preserving DAE model of the power system, the generators are modeled using the rotational dynamics provided by the classical swing equation, and the loads are modeled as constant PQ loads (considered power distribution centers), forming the system equations:

$$\begin{aligned} f^I : \dot{\delta}_i - \omega_i &= 0 \\ f^{II} : \dot{\omega}_i + \frac{D_i}{M_i}(\omega_i) + \frac{1}{M_i} P_{G_i}(\delta, \theta, V, N) &= \frac{P_{M_i}}{M_i} \\ f^{III} : P_j^* - P_j(\delta, \theta, V, N) &= 0 \\ f^{IV} : Q_j^* - Q_j(\delta, \theta, V, N) &= 0 \end{aligned} \quad (6)$$

$$N : Y_{cd} = G_{cd} + jB_{cd}$$

$$\begin{aligned} i &= 2 \dots n \text{ generators; } j = n+1 \dots m \text{ loads;} \\ c, d &= 1 \dots n+m \end{aligned}$$

where δ_i , M_i , D_i and P_{M_i} are the internal angle, inertia, damping and constant mechanical power of the i_{th} generator respectively, and θ_j and V_j are the j_{th} load bus angle and voltage respectively. The desired power demand on the j_{th} load bus is denoted $S^* = P^* + jQ^*$. The system has the form of (1), with $f(\cdot)$ in (1) comprised of f^I and f^{II} and $g(\cdot)$ in (1) comprised of f^{III} and f^{IV} , and with respect to the form given in (2):

$$\begin{aligned} F(\dot{x}, x, N) &= [f^I \ f^{II} \ f^{III} \ f^{IV}]^T \\ x &= [\delta_i, \omega_i, \theta_j, V_j], \quad u = \frac{P_{M_i}}{M_i} \end{aligned} \quad (7)$$

The available measurements are all assumed as real power branch flows, given as:

$$h(x, N) = \{P_{cd}(x, N)\} \quad (8)$$

This system can be further modified to incorporate generator exciter dynamics or dynamics in the system loads. The observability formulation for these variations was discussed in [3-6], and the addition of other types of generator and load models (voltage dependent loads for example) will impact the construction of the observability Jacobian only. The methodology for obtaining the Jacobian, the observability conditions and the degree of observability measure is consistent. Also, it should be noted that in (6) generator bus 1 was arbitrarily selected as the reference bus, yielding $\delta_i: \delta_i - \delta_1$ and $\theta_j: \theta_j - \delta_1$.

B. Observability Metric

To quantify the observability of the system during a variation, a measure of observability is introduced, defined as:

$$\eta^l = \frac{\lambda_{\max}(J_o)}{\lambda_{\min}(J_o)}, \quad l = 1 \dots L \quad (9)$$

where λ_i are the singular values of the observability Jacobian obtained via a singular value decomposition at each point of interest l . The maximum number of L , is dictated by the convergence of the numerical solvers used for either static studies (points along PV Curve), or dynamic studies (length of time window in a time domain simulation).

The degree of observability γ is defined as:

$$\gamma = \max \{\eta^l\} \quad l = 1 \dots L \quad (10)$$

Based on the formulation of this measure, a smaller numerical value of γ is preferred – a higher number indicates that the observability Jacobian is becoming singular.

III. APPROACH

To determine all the singularities of the observability Jacobian, a symbolic computation approach is used. Also, time domain simulations are used to track the observability of the system along the system state trajectories, as these unobservable regions are approached. A brief description of both the symbolic and numerical approaches is provided.

A. Symbolic Approach

The symbolic approach examines the observability criteria as a function of the system state space. In particular, the examination is focused on finding where in the state-space the observability Jacobian undergoes rank deficiencies. In essence, by examining where observability is lost, all other points in the state-space are assumed to be observable. This is assumed, rather than guaranteed, because of the performance of the symbolic tools in evaluating rank deficiencies. Namely their performance in locating higher order degeneracies in the Jacobian is of question. For the particular system examined, the symbolic tools were able to capture higher order degeneracies. This technique is powerful in the sense that it provides the global solutions where the system is unobservable, however it is limited by the computational capability of the symbolic solvers, and hence, is limited to the size of the system that can be evaluated. The symbolic approach process is outlined in Figure 1.

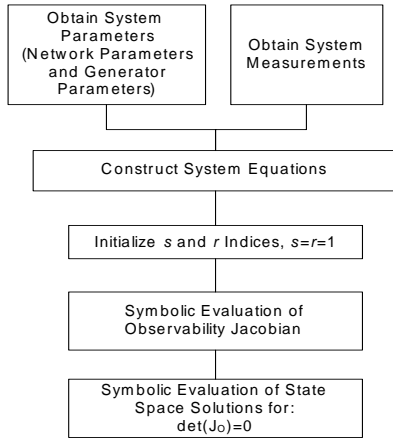


Fig 1. Investigating Observability using Symbolic Tools

B. Numerical Approach

The numerical approach consists of two separate cases:

- Static Cases – Evaluating observability for operating points along system PV Curves
- Dynamic Cases – Evaluating the observability criterion along trajectories of the system states

The general approach in evaluating these criteria and determining the appropriate s and r to render the system observable is outlined in Figure 2.

For the static cases, the solution of the system PV curves is accomplished in an iterative fashion using the Newton-Raphson (NR) and Newton-Raphson-Seydel (NRS) algorithms [9]. When the NR algorithm fails, the NRS algorithm is used to obtain the data points near and around the nose point of the PV curve, as illustrated in Figure 3.

For the numerical cases, the ode15s DAE solver was used in the Matlab/Simulink environment to generate the time domain simulations of interest.

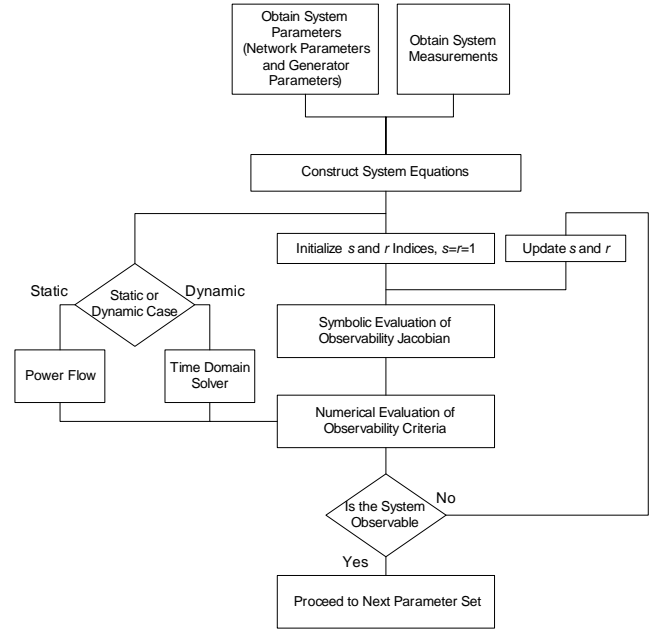


Fig 2. Flow Diagram of the Numerical Approaches in Determining Observability

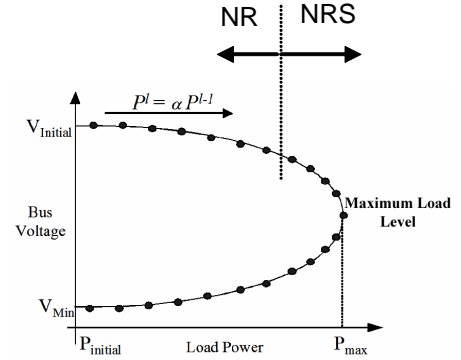


Fig 3. Typical Power System PV Curve

IV. SIMULATION RESULTS

A. Sample System

To illustrate the symbolic approach for obtaining the unobservable regions, a 3-bus power system depicted in Figure 4, with corresponding system parameters in Table 1, was used. There are two sets of results – considering two different measurements, P_{12} and P_{32} . In both cases, $r=s=1$, and the singularity of the Jacobian is investigated by solving the following relationship symbolically:

$$\det(J_o) = 0$$

For the selected system, the observability Jacobian has the general form provided in (11), and the states of the system are given as:

$$x = [\theta_2, \omega_2, \theta_3, V_3]$$

$$J_o = \begin{bmatrix} 0 & -1 & 0 & 0 & 1 & 0 & 0 & 0 & 0 & 0 \\ j_{2,1} & j_{2,2} & j_{2,3} & j_{2,4} & 0 & 1 & 0 & 0 & 0 & 0 \\ j_{3,1} & 0 & j_{3,3} & j_{3,4} & 0 & 0 & 0 & 0 & 0 & 0 \\ j_{4,1} & 0 & j_{4,3} & j_{4,4} & 0 & 0 & 0 & 0 & 0 & 0 \\ 0 & 0 & 0 & 0 & 0 & -1 & 0 & 0 & 1 & 0 \\ j_{6,1} & 0 & j_{6,3} & j_{6,4} & j_{6,5} & j_{6,6} & j_{6,7} & j_{6,8} & 0 & 1 \\ j_{7,1} & 0 & j_{7,3} & j_{7,4} & j_{7,5} & 0 & j_{7,7} & j_{7,8} & 0 & 0 \\ j_{8,1} & 0 & j_{8,3} & j_{8,4} & j_{8,5} & 0 & j_{8,7} & j_{8,8} & 0 & 0 \\ j_{9,1} & 0 & j_{9,3} & j_{9,4} & 0 & 0 & 0 & 0 & 0 & 0 \\ j_{10,1} & 0 & j_{10,3} & j_{10,4} & j_{10,5} & 0 & j_{10,7} & j_{10,8} & 0 & 0 \end{bmatrix} \quad (11)$$

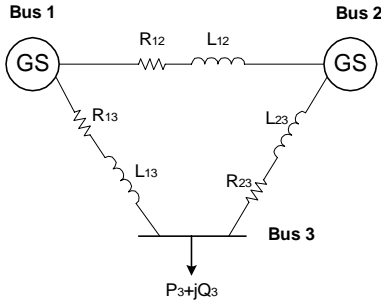


Fig. 4. Sample 3-bus Power System

TABLE I
SYSTEM PARAMETERS FOR SAMPLE 3-BUS POWER SYSTEM

Line	R	X	D=1
1-2	.0194	.0592	M=1
2-3	.0470	.1980	
1-3	.054	.2230	
Bus	P ^{initial}	Q ^{initial}	V ₁ =1.06
2	.1830	-	V ₂ =1.04
2	-.9420	.0440	

B. Symbolic Results – Loss of Observability

By computing the determinant symbolically and equating it to zero, there are 6 solutions for x which yield rank deficiencies (Table II). In analyzing the solutions, and keeping in mind the significance of the respective system state assignments, the first five solutions are not considered physically realizable. For Solution 1, the bus voltage at the load bus would have to go to zero, meaning the generators are either offline or the topology of the system has changed (due to a fault on Bus 3, or faults on both lines connecting Bus 3 to the two generator buses). Similarly, for Solutions 2-5, the angle difference between generator 1 and the load bus is 90 degrees, which would indicate a phase instability in the system. Therefore, for the first five solutions, one can assume that the system will be smoothly observable for all perturbations that do not cause these specific system instabilities, and that one measurement (P_{32}) is sufficient for the system to be smoothly observable. The only solution of interest now is Solution 6, which represents the load bus voltage as a function of the two bus phases in the system. Similarly for the case of a measurement P_{12} (Table III), the

first 2 solutions represent either a fault on bus 3, or a phase instability, and the third solution provides the bus voltage as a function of the bus phases.

TABLE II
SYSTEM OBSERVABILITY IS LOST AND THE CORRESPONDING RANK OF THE OBSERVABILITY JACOBIAN – P_{32}

Solution	x_1	x_2	x_3	x_4	Rank
1	x_1	x_2	x_3	0	6
2	0	x_2	$\pi/2$	x_4	8
3	0	x_2	$-\pi/2$	x_4	8
4	π	x_2	$\pi/2$	x_4	8
5	π	x_2	$-\pi/2$	x_4	8
6	x_1	x_2	x_3	$f(x_1, x_3)$	8

TABLE III
SYSTEM OBSERVABILITY IS LOST AND THE CORRESPONDING RANK OF THE OBSERVABILITY JACOBIAN – P_{12}

Solution	x_1	x_2	x_3	x_4	Rank
1	x_1	x_2	x_3	0	6
2	$\pi/2$	x_2	x_3	x_4	8
3	x_1	x_2	x_3	$f(x_1, x_3)$	8

Examining Solution 6 of Table II and Solution 3 of Table III, and similar solutions for a lossless system, an unobservable region can be constructed, given a range for the bus angles is specified. To examine the physical interpretation of these solutions, the initial operating point in Table I is selected with:

$$x = [-.0869, 0, -.2220, 1.01]$$

and an arbitrary PV curve is constructed (Figure 5). Using the phase quantities dictated by the PV curve, the relationship of the load bus voltage to the phase difference between bus 2 and 3 is examined and compared to the results for the load bus voltage obtained using the PV curve. The phase difference was used as a parameter to condense the problem into 2-D.

Examining Figure 6, the solution for the load bus voltage magnitude intersects the unobservable solutions obtained from Tables II and III, and using the information obtained by the PV curve, this intersection corresponds to the maximum load point of the system (magnified in Figure 7). This result is consistent with all the obtained solutions, and is invariant to the selected measurement, and to the implication of a lossless or lossy system. Due to the symmetry of the system topology used, the results for P_{13} are the same as those for P_{32} and are not included.

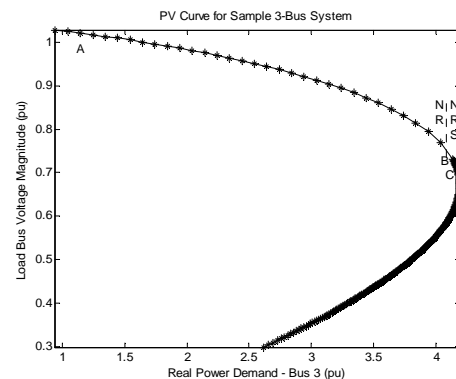


Fig 5. Arbitrary PV Curve of 3-Bus System

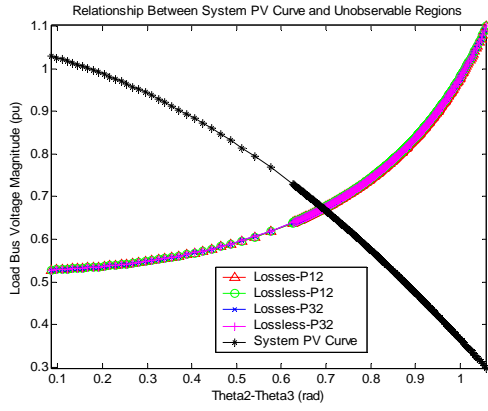


Fig. 6 Relationship Between System PV Curve and Unobservable Solutions

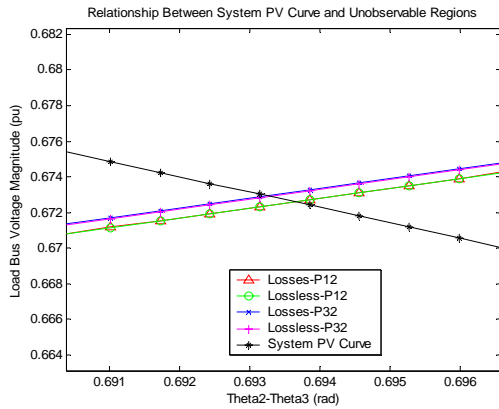


Fig. 7 Relationship Between System PV Curve and Unobservable Solutions – Intersection Magnified

Therefore, for the selected system, a duality exists between the loss of observability and the voltage stability problem. At the maximum load point, the system is unstable and unobservable. This is also present with cases of phase instability, represented by the solutions in Table II and III, where large phase differences exist between the generator and load bus.

C. Dynamic Simulations

Because of the limitations with symbolic tools, analyzing larger systems are not possible without the introduction of numeric methods. However, unlike the symbolic approach which yielded the entire family of unobservable solutions, the numerical approaches are constrained to only approach a point of interest. To illustrate that the numerical results are consistent with the answers from the symbolic computations, three arbitrary points are selected along the PV curve (points A, B and C in Figure 5, given in Table IV). A 40% perturbation is applied to the generator phase at each point, and the resulting time domain waveforms are extracted (waveforms provided in Appendix). These time domain waveforms are then used to analyze the observability index

along the trajectories of the system states. It is expected that the observability index for the trajectories associated with point C will be higher. By repeating this process for the entire set of points along the PV curve, a threshold on the observability index was obtained ($\gamma \approx 600$), and the individual γ is provided in Table V, for the perturbation level of 40% on the generator phase.

TABLE IV
ARBITRARY POINTS ALONG PV CURVE CHOSEN FOR TIME DOMAIN SIMULATIONS

Point	x_1	x_3	x_4	P_2	P_3	Q_3
A	-.0076	-.1167	1.0218	.3830	-1.1420	.0440
B	.0461	-.5918	.7196	3.4006	-4.1596	.0440
C	.0047	-.6274	.6911	3.4302	-4.1892	.0440

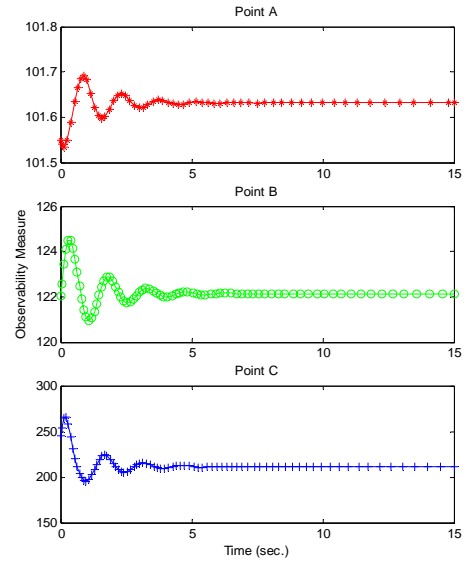


Fig. 8. Observability Measure along State Trajectories for Points A, B and C.

TABLE V
OBSERVABILITY INDEX FOR EACH SET OF TRAJECTORIES INITIATED FROM POINTS A, B AND C

Point	γ
A	101.6915
B	124.4947
C	265.4845

As expected, the trajectories produced from the points closer to the nose point produced larger index values, indicating that the system is becoming less observable, and they are consistent with the results obtained using the symbolic approach. However, at no point does the system become unobservable in a numerical sense. The observability criteria of Equation 5 are satisfied for all the points along the PV curve, and system trajectories for this system. A closer examination indicates that a quantitative change is occurring as the system is approaching the maximum load point. This is evident when examining the minimum singular value of the observability Jacobian for each point along the PV curve. As

illustrated in Figure 9, the value approaches zero at the maximum load point. From a numerical standpoint, the system is still observable, and this problem is hence transformed into a numerical sensitivity issue. The appropriate selection of thresholds on γ provides a better depiction; however, this process involves extensive system simulations to set these thresholds.

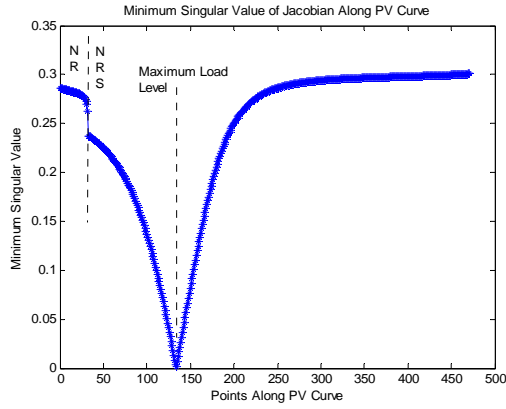


Fig 9. Minimum Singular Value of Jacobian Along PV Curve

V. CONCLUSIONS

Singularities of the observability Jacobian correspond with system singularities that are typically associated with phase and voltage stability problems in power systems. This duality can be exploited by using the observability index as a system metric capable of forecasting both the stability and observability classifications of a power system. The dual use of a single metric is very encouraging. In the case of system stability, since the common points are fewer than the entire family of unstable points for a system, this metric would serve as a necessary but not sufficient condition.

VI. APPENDIX

Time domain simulations for the sample system considered in previous section are provided in Figures 10-12.

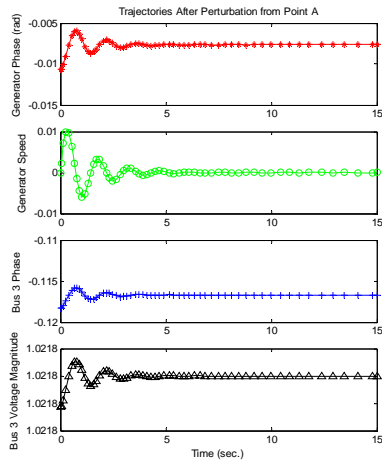


Fig 10. Trajectories After Perturbation from Point A

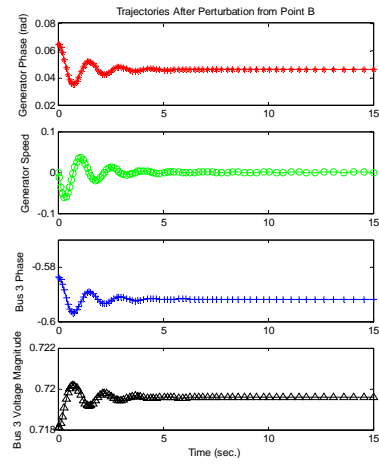


Fig 11. Trajectories After Perturbation from Point B

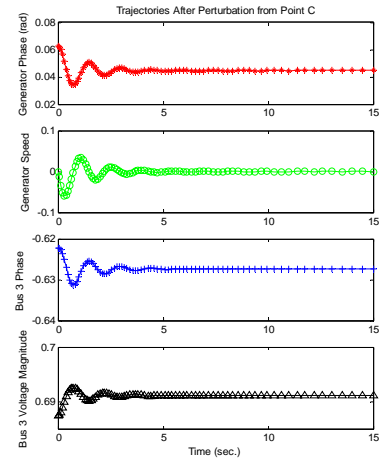


Fig 12. Trajectories After Perturbation from Point C

VII. REFERENCES

- [1] K. L. Butler-Perry, N. D. R. Sarma, I. V. Hicks, "Service Restoration in Naval Shipboard Power Systems", *IEEE Proceedings on Generation, Transmission and Distribution*, Vol. 151, Issue 1, pp95-102.
- [2] National Research Council, Technology for the United States Navy and Marine Corps 2000-2035-Becoming a 21st Century Force, Volume 2: Technology, National Academic Press, Washington, 1997.
- [3] C. J. Dafis, "An Observability Formulation for Nonlinear Power Systems Modeled as Differential Algebraic Systems," Ph.D. Dissertation, Dept. Elect. & Comp. Eng., Drexel University, Philadelphia, Feb. 2005.
- [4] C. J. Dafis, C. O. Nwankpa, "Characteristics of Degree of Observability Measure for Nonlinear Power Systems", in *Proc. 2005 Hawaii International Conference on System Science*.
- [5] C. J. Dafis, C. O. Nwankpa, "A Nonlinear Observability Formulation for Power Systems Incorporating Generator and Load Dynamics", in *Proc. 2002 IEEE Conference on Decision and Control*, Vol.3, pp.245-2449, 2002.
- [6] C. J. Dafis, C. O. Nwankpa, "Examining Characteristics of an Observability Formulation for Nonlinear Power Systems", in *Proc. 2003 IEEE International Symposium on Circuits and Systems*, Vol. 3, pp.395-398.
- [7] P.W. Sauer, M. A. Pai, *Power System Dynamics and Stability*, Prentice Hall, Upper Saddle River, New Jersey, 1998.
- [8] W. J. Terrell, "Observability of Nonlinear Differential Algebraic Systems", *Circuits, Systems, and Signal Processing*, Vol. 16, No.2, 1997, pp.271-285.
- [9] R. Seydel, *Practical Bifurcation and Stability Analysis – From Equilibrium to Chaos*, Springer-Verlag, New York, 1994.